Kangas, H., Pöhler, T., Heikkurinen, A. and Kleen, M. (2004). Development of the mechanical pulp fibre surface as a function of refining energy. Journal of Pulp and Paper Science 30 (11): 298-306.

Development of the Mechanical Pulp Fibre Surface as a Function of Refining Energy

H. KANGAS, T. PÖHLER, A. HEIKKURINEN and M. KLEEN

*Thermomechanical pulps were produced by refining spruce wood (*Picea abies*) chips at various specific energy consumptions. The surface morphology and chemistry of isolated fibres were studied. Different types of fines, i.e. flakes and fibrils, were characterized chemically to obtain information about their origin in the fibre wall. After the two mainline refining stages, 85% of the S2 fibre wall layer was revealed. The lignin coverage of mainline fibres was higher and the surface content of polysaccharides was lower than that of reject line fibres. Surface extractives were almost totally removed during screening. At a low energy consumption, fibrillar fines were formed from the outer fibre wall layers (P+S1), but the content of secondary wall material increased as a function of refining energy. During mainline refining, the flake-like fines originated from compound middle lamella (ML+P) while, in reject refining, they were also released from the outer secondary wall layer (S1).*

*Nous avons produit des pâtes thermomécaniques en raffinant des copeaux d'épinette (*Picea abies*) à divers degrés de consommation d'énergie spécifique. Nous avons étudié la morphologie de la surface et la chimie de fibres isolées. Différents types de fines (flocons et fibrilles) ont été caractérisés chimiquement afin d'obtenir des données sur leur origine dans la paroi de la fibre. Quelque 85 % de la couche S2 de la paroi est apparue après les deux premiers étages du circuit de raffinage principal. Le recouvrement par la lignine des fibres du circuit principal était plus étendu et la teneur superficielle en polysaccharides était inférieure à celle des fibres du circuit des refus. Les matières extractives superficielles ont été presque totalement éliminées lors du classage. À une faible consommation d'énergie, les fines fibrillaires étaient formées à partir des couches extérieures de la paroi des fibres (P+S1), mais la teneur en matière de la paroi secondaire s'est accrue comme fonction de l'énergie de raffinage. Pendant le raffinage dans le circuit principal, les fines floconneuses provenaient de la lamelle mitoyenne composée (ML+P), tandis que pendant le raffinage des refus, elles se détachaient aussi de la couche extérieure de la paroi secondaire (S1).*

INTRODUCTION

The high demands placed on the quality of mechanical printing papers have made the properties of mechanical pulps increasingly important. At the same time, the entire manufacturing process needs to be as cost-effective as possible. In this, process development plays a key role. The physical and chemical properties of mechanical pulps and their influence on paper quality have been much studied, but less attention has been given to the pulps' surface properties. Many studies have been conducted on the development of fibre properties during the pulping process, including the development of surface properties [1–6]. The surface properties of papermaking pulps are very important, since they may influence fibre charge, fibre bonding, wettability, adsorption, adhesion and consumption of papermaking chemicals. Pulp surface properties can also influence paper manufacturing and finishing operations such as coating and printing.

The refining process can be divided into two stages: fibre separation and fibre development, which can occur simultaneously [7]. In the fibre separation stage, wood chips are

JPPS
H. Kangas, T. Pöhler,
A. Heikkurinen and M. Kleen
KCL
P.O. Box 70
FIN-02151 Espoo, Finland
(heli.kangas@kcl.fi)

broken into smaller particles. Fibre development proceeds via delamination and peeling of the fibre surface. Outer fibre wall layers, i.e. primary wall (P) and outer secondary wall (S_1), are peeled off, leaving the inner secondary wall (S_2) exposed. The properties of fibre surfaces change naturally as refining progresses. In a two-stage refining process, fibre separation and fibre development usually occur in the first stage, and fibre development continues as the main process during the second stage and during reject refining also.

Fines material is generated during both fibre separation and fibre development, its physical and chemical properties depending on its origin in the fibre wall. Lignin-rich flake-like fines and ray cells arise mainly during the first phases of refining, while fibrils containing more cellulose are formed during the peeling of cellulose-rich inner fibre wall layers [8]. The properties of fines greatly influence their effect on paper quality, since flakes are known to enhance the light-scattering properties of paper, while fibrils are important for strength properties [9].

The morphology of mechanical pulp fibre surfaces can be studied by microscopy, for example with a scanning electron microscope (SEM) [1,3,10,11]. A SEM equipped with a field emission gun (FE–SEM) produces images of fibre surfaces at high magnifications and can be used to study fine surface details. The surface chemical properties of mechanical pulps have been studied traditionally by means of electron spectroscopy for chemical analysis (ESCA, also called X-ray photoelectron spectroscopy) [12–19]. ESCA can provide information about the surface down to a depth of 5–10 nm. Time-of-flight secondary ion mass spectrometry (ToF–SIMS) is even more surface sensitive than ESCA, giving information from the first molecular layer of the surface (~1 nm). ESCA can be used to obtain quantitative information about the surface coverage of extractives, lignin and polysaccharides on pulp and paper surfaces, while ToF–SIMS yields only qualitative or semi-quantitative data on the surface composition [20–22]. However, ToF–SIMS gives detailed structural information about the surface compounds and thus can complement the information given by ESCA.

The aim of this work was to find out how the fibre surface changes, both structurally and chemically, as refining proceeds. FE–SEM was used to study surface morphology and ESCA and ToF–SIMS were used to evaluate the surface chemical properties. Another aim was to find out how an increase in refining energy influences the fines fraction. Information about the development of fibre and fines properties during refining will help in designing a more optimal refining process.

MATERIALS AND METHODS

Pulp Samples

Spruce wood chips were refined on the pilot scale into thermomechanical pulp (TMP). Thick-walled Norway spruce (*Picea abies*) from a slow-growth forest stand ~60 years old was used as raw material. Refining was carried out on the pilot scale at KCL, Espoo, Finland. The refiner used was a Sunds Defibrator, Jylhä Oy, Valkeakoski, Finland RGP 42 refiner operated with 112 cm (44") refiner segments. The preheating time was ~40 s and the refining was performed in two stages in a single disc refiner using a rotational speed of 1500 rpm. Prior to screening, the pulp was hot disintegrated in a pulper using fresh steam. The temperature during hot disintegration was a minimum of 72°C in the beginning, the time 45 min and the pulp consistency ~5%. The pilot screen used was Valmet-Tampella (Metso, Jyväskyla, Finland) TAP 50 and the screen basket was a wedge wire basket with a slot width/contour height of 0.10/0.8 mm in the first screening stage and 0.10/0.65 mm in the second screening stage. The pulp consistency during screening was 1% and the reject rate 50%. The reject pulp was refined further in two stages up to a total energy consumption of 4.9 MWh/t. In the second reject refining stage, three different energy levels were used. Six pulp samples from different refining stages were taken for further analysis. Pulps were stored frozen until needed. The refining process and the conditions used are shown in Fig. 1. Pulps from mainline refining are marked with the letter A (A1 and A2) and pulps from reject refining with the letter B (B1–B4).

Basic pulp properties were tested. Wet disintegration was performed according to standard EN ISO 5263 [23], dry matter content was determined according to EN 20638 [24] and Canadian standard freeness (CSF) according to ISO 5267-2 [25]. Bauer-McNett fractions were determined according to Scandinavian standard SCAN-M 6:69 [26]. Fibre length was measured using a Kajaani (Metso Automation, Kajaani, Finland) FS-200 instrument.

Some properties of the Bauer-McNett fractions were also studied. Fibre wall thickness was measured by light microscopy using semi-automatic image analysis from a wet, longitudinal fibre preparation (+14 fraction). Fibre width and lumen width were measured automatically by image analysis at one representative location in a fibre.Two hundred fibres were measured in each analysis. Fibre wall thickness was calculated from Eq. (1).

$$\text{Fibre wall thickness} = (\text{fibre width} - \text{lumen width})/2 \quad (1)$$

Coarseness was determined from the 14/28 fraction using the Kajaani FS-200. Development of the middle fraction was measured as the specific filtration resistance of the 48/200 fraction. Pulp slurry (consistency C = 0.01%) was filtered through a 100 mesh wire (A = 19.6 cm^2) at a constant rate (q = 20–30 mL/s) and the time (t) needed to reach a 10 kPa pressure difference (ΔP) across the pulp pad was measured. The S value describing the filtration resistance of the pulp was calculated from Eq. (2), where η is the viscosity of water.

$$S = \frac{A^2 \Delta P}{\eta q^2 C t} \quad (2)$$

The character of the fines was evaluated as the specific sedimentation volume of the –200 mesh fraction. This reflects the proportion of fibrillar fines in the fines fraction. The fines suspension (375 mg o.d.) was centrifuged (10 min, 4000 rpm) and water containing 30 mg/L $CaCl_2 \cdot H_2O$ and 120 mg/L Na_2SO_4 was added. Air was removed from the slurry by suction. The sedimented volume was read after 24 h.

Isolation of Fines

TMP was hot disintegrated (85°C, 10 min) and diluted to 0.5% consistency with distilled

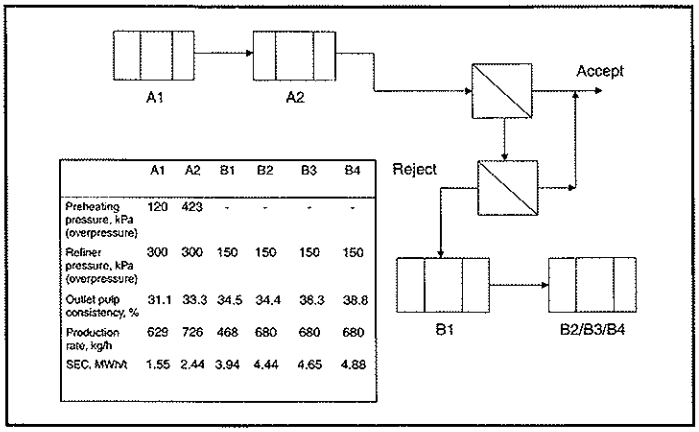

	A1	A2	B1	B2	B3	B4
Preheating pressure, kPa (overpressure)	120	423	-	-	-	-
Refiner pressure, kPa (overpressure)	300	300	150	150	150	150
Outlet pulp consistency, %	31.1	33.3	34.5	34.4	38.3	38.8
Production rate, kg/h	629	726	468	680	680	680
SEC, MWh/t	1.55	2.44	3.94	4.44	4.65	4.88

Fig. 1. Refining of TMP samples.

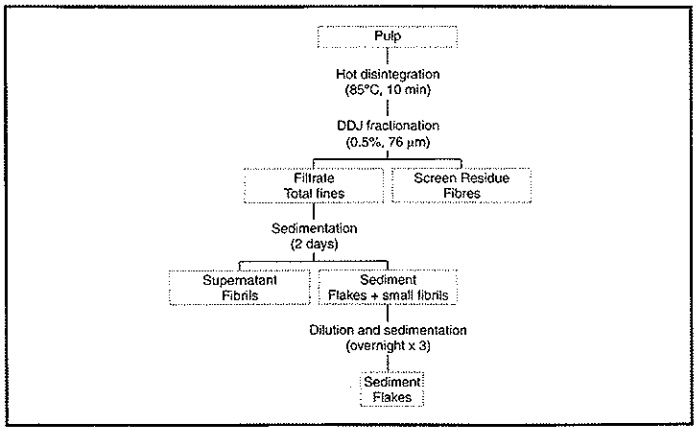

Fig. 2. Fractionation procedure used to separate fibres and various types of fines.

water. The pulp slurry was passed on to the dynamic drainage jar (DDJ), which was equipped with a 200 mesh (76 μm) wire and propeller stirring, and the valve was opened. The suspension was washed with distilled water until 10 L of slurry had been collected. The fines fraction passed through the wire, while the fibres were retained on the screen. The various types of fines, i.e. fibrillar and flake-like fines, were separated further from each other using sedimentation. The total fines fraction was allowed to sediment first for two days, after which the supernatant enriched in fibrillar fines was collected. Excess water was removed from the fibrils by centrifugation (5500 rpm, 15 min). The sediment was again diluted to 10 L with distilled water. Next morning, the clear supernatant was removed and discarded and the volume was again adjusted to 10 L. This washing of the sediment was repeated three times. The fractionation procedure is outlined in Fig. 2. The final sediment contained flake-like fines, including ray cells, and was quite free from fibrillar material. The fractionation results of both fines fractions were evaluated by image analysis.

Image Analysis

Various fines fractions were studied with an image analyzer developed by Luukko et al. [9] and improved further by Metso Corp., Finland. The image-analysis program classifies the fines particles into fibrillar and non-fibrillar material and calculates the mass proportion of fibrillar material. The program also identifies particles having a rectangular shape, which is typical of ray cells, and computes their mass proportion. The mass proportion of flakes, other than ray cells, was calculated as the difference (100 - fibrils - ray cells)%.

Gross Chemical Analysis

The amount of acetone-extractable material (%) was determined according to standard SCAN-CM 49:93 [27]. An amount of 0.5–5 g of sample was extracted with 70 mL of acetone for 1 h using a Soxtec apparatus. The solvent was evaporated and the extraction residue was dried in a drying oven at 40°C and weighed.

Lignin was determined according to a modified TAPPI test method T 222 [28]. The primary hydrolysis was performed by adding 2 mL of 72% H_2SO_4 to 200 mg of finely ground, extractive-free, freeze-dried sample and incubating the slurry for 1 h at 30°C. In the secondary hydrolysis, 56 mL of water was added to the sample and the suspension was kept in an autoclave at 120°C for 1 h. The supernatant was removed by filtration and the sediment washed several times with water. The sediment was then dried at 105°C for 2 h and weighed to give the content of gravimetric lignin. Acid-soluble lignin was determined by measuring the absorbency of the solution at 203 nm, using 128 L/g·cm as the absorptivity coefficient.

Cellulose was determined according to a modified TAPPI test method T 249 [29]. The supernatant removed after primary and secondary hydrolysis was combined with the washing water, and the solution was diluted to 200 mL with water. An amount of 4 mL of this solution was taken for carbohydrate analysis and 1 mL of 2 μg/L D-fucose was added as the internal standard. The monosaccharide content was determined by anion exchange liquid chromatography using pulsed amperometric detection. The amount of cellulose was calculated from the glucose units using a factor of 0.9.

The chemical composition of hemicelluloses and pectins was determined by acid methanolysis. The advantage of acid methanolysis over acid hydrolysis is the simultaneous determination of all uronic acids with neutral sugars [30]. An amount of 2 mL of 2 mol/L HCl in anhydrous methanol was added to 10 mg of freeze-dried sample. The sample was kept at 100°C for 3 h, after which pyridine and sorbitol were added as internal standards. The samples were evaporated to dryness and transferred to gas chromatography vials with sorbitol. The samples were silylated and kept at 70°C for 3 h. The silylated derivatives were analyzed using gas chromatography/mass spectrometry according to [31]. The sugar units determined were arabinose (Ara), rhamnose (Rha), xylose (Xyl), 4-*O*-methylglucuronic acid (4-*O*-MeGlcA), mannose (Man), galactose (Gal), galacturonic acid (GalA), glucuronic acid (GlcA) and glucose (Glc). Acetylgalactoglucomannan was determined as Ac:Gal:Glc:Man 1:0.5:1:4 and converted to polysaccharide using a factor of 0.9, and xylan as Ara:4-*O*-MeGlcA:Xyl 1.3:2:10 and converted to polysaccharide using a factor of 0.88 [32]. Arabinogalactan was determined as GlcA:Ara:Gal 0.8:1:3.6 [33] and converted to polysaccharide using a factor of 0.9. The residual arabinose was calculated as arabinan using the factor 0.88. Rhamno- galacturonan was calculated using the factor 0.9. The content of pectins was calculated as the sum of acidic and neutral pectins, i.e. the sum of galacturonans, arabinans and galactans.

FE–SEM Analysis

The morphology of pulp fibres was characterized using a FE–SEM (Jeol JSM 6335F) at Top Analytica Ltd., Turku, Finland. A very low acceleration voltage (1 kV) was used. Fibres from the +14 fraction were prepared for FE–SEM analysis by performing a gradual solvent exchange (water:ethanol) prior to drying in a critical-point dryer. This was done to avoid changes in the structure due to surface tension. However, some shrinking of the fibres was seen. Fibres were sputter coated with a thin layer of Au–Pd.

A manual method for the quantitative assessment of the character of fibre surfaces was also developed. The lengths of areas with the S_2 layer exposed were measured and compared to the total fibre length examined. From each pulp sample, 50 single, critical-point dried fibres from the +14 Bauer-McNett fraction were measured in this way by FE–SEM. The total fibre length examined per pulp sample was 100 mm.

ESCA Analysis

Small sheets were prepared from the various fractions for ESCA analysis. The sheets were made in a glass funnel on a 20 μm nylon screen, dried between blotters and stored in a freezer. Part of each sheet was extracted with acetone according to standard SCAN-CM 49:93 [27]. The ESCA analyses were performed with a Kratos Analytical AXIS 165 high-resolution electron spectrometer at the Center for Chemical Analysis, Helsinki University of Technology, Espoo, Finland. Sample sheets were measured before and after extraction using monochromatic Al $K\alpha$ irradiation (12.5 kV, 8 mA). Both survey scans in the range 0–1100 eV (1 eV step, 80 eV analyzer pass energy) and high-resolution spectra of C 1s and O 1s regions (0.1 eV step, 20 eV pass energy) were recorded at three different locations for each sample. The area of analysis was ~1 mm^2 and the depth of analysis 2–10 nm. The insulating sample surfaces were neutralized during the measurement with low-energy electrons. The

TABLE I
BASIC PULP PROPERTIES

	A1	A2	Reject	B1	B2	B3	B4
Pulp properties							
CSF, mL	340	122	410	100	60	50	37
Fibre length, mm	1.96	1.85	2.24	2.06	1.92	1.92	1.8
Bauer-McNett +14, %	36.8	30.5	51.5	33.3	38.1	37.3	35.8
Bauer-McNett +28, %	21.6	20.8	21.4	21.3	19.6	20.6	19.2
Bauer-McNett +48, %	12.4	12.1	11.0	11.9	11.3	10.7	10.4
Bauer-McNett +200, %	10.8	12.5	8.8	15.6	13.0	13.7	14.7
Bauer-McNett –200, %	18.4	24.1	7.3	17.9	18.0	17.7	19.9
Properties of fractions							
Fibre wall thickness (+14, average), μm	5.9	5.8	6.6	5.0	4.9	4.8	5.0
Coarseness (14/28), mg/m	0.417	0.259	0.264	0.232	0.225	0.218	0.199
Specific filtration resistance (48/200), 10^{-8} m/kg	184	397	452	612	1122	1592	974
Sedimentation volume (–200), dm^3/kg	420	520	560	580	610	620	610

surface coverage (% of area) of lignin and extractives was calculated from the averaged C-C percentages in high-resolution C 1s spectra [34]. The surface coverage of polysaccharides was calculated as the difference (100 - coverage of lignin - coverage of extractives)%.

ToF–SIMS Analysis

Small sheets that had not been extracted were used for ToF–SIMS analysis. The instrument used was a PHI TRIFT II ToF–SIMS from Physical Electronics, Eden Prairie, MN, USA, at Top Analytica Ltd., Turku, Finland. ToF–SIMS spectra in positive and negative ion modes were acquired using a Ga liquid metal ion gun with 15 keV primary ions in bunched mode over the mass range 2–2000 m/z. The primary ion current was 600 pA, time per channel 0.138 ns, analysis area 200 x 200 μm and acquisition time 5 min. Analytical charge compensation was used for insulating samples. The calculated ion dose was $2.7 \cdot 10^{11}/cm^2$, which ensured static conditions during data acquisition. Three replicate runs were made for each sample. Peak identification in ToF–SIMS spectra was based on model compound analysis [35]. The peaks identified were integrated and normalized to the total intensity of the spectrum.

RESULTS AND DISCUSSION

Basic Pulp Properties

The basic pulp properties, including those of the reject pulp, are shown in Table I. The properties related to the development of fibre surface, such as fibre wall thickness and coarseness, and to the quality of middle fraction or fines, such as specific filtration resistance and sedimentation volume, are discussed further here.

Fibre wall thickness decreased generally as specific energy consumption (SEC) increased. The reduction in fibre wall thickness indicates that fibre development was taking place by the peeling of the fibre wall layers.

The coarseness was high after the first refining stage (A1), and decreased linearly as a function of SEC as material was peeled off from the fibre wall.

Specific filtration resistance has been shown to correlate with the bonding ability of the middle fraction (48/200) [36]. It was found to increase as a function of SEC, but a decrease occurred at the highest energy level in the reject line. An increase in filtration resistance indicates that more fibrillar material with good bonding properties was created at higher energy consumption, while a decrease shows that, at the highest energy level, the refining action was changed and bulkier material with poorer bonding properties was generated and passed into the middle fraction.

The content of fines (Bauer-McNett –200 fraction) increased during mainline refining and the first reject refining stage. Fewer fines by weight were generated during the second stage of reject refining, except at the highest energy level (B4), where the content of fines increased slightly.

Sedimentation volume has been shown to correlate with the length of fines particles [8] and their bonding ability [37]. Fibrils are known to have good bonding ability and, thus, the higher the sedimentation volume, the higher the fibrillar content [37]. The sedimentation volume increased as a function of refining energy, apart from a slight decrease during the last stage of reject refining, indicating that less fibrillar material was generated there.

Composition of Fines Fractions

Increased sedimentation volume indicated that the content of fibrillar fines increased as a function of refining energy, which is in agreement with earlier studies [8]. However, such a correlation was not seen between the content of fibrillar fines given by the image analyzer and the SEC (Table II). A difference in the content of fibrillar fines was seen between the mainline pulps and the reject refined pulps. Also, the content of fibrils was higher after the second stage of reject refining than after the first stage. Thus, the relationship between the content of fibrillar fines given by the image analyzer on one hand and the sedimentation volume on the other appears not to be straightforward.

The content of flake-like fines, i.e. ray cells and pieces of middle lamella and fibre wall, was higher in the mainline pulps than in the reject line pulps. The reject line pulps still contained a significant amount of flake-like fines, which probably were formed from the remaining outer cell wall layers ($P+S_1$).

The total fines fraction was fractionated into fibrillar and flake-like fines. Fractionation was successful, since the content of fibrils was found to be between 80 and 84% in the enriched fibrillar fractions (Table II). The enriched flake fraction contained mainly flake-like material (79–92%), of which 15–25% was classified as ray cells.

TABLE II
COMPOSITION OF FINES FRACTIONS

	Fibrils	Ray cells	Flakes
Total fines			
A1	40	9	51
A2	41	8	51
B1	50	6	43
B2	53	4	43
B3	53	5	42
B4	53	6	41
Enriched fibrillar fines			
A1	81	1	18
A2	84	1	16
B1	84	1	16
B2	81	1	18
B3	83	1	17
B4	80	1	19
Enriched flake-like fines			
A1	21	15	65
A2	8	25	67
B1	12	15	73
B2	11	18	71
B3	11	17	72
B4	11	15	74

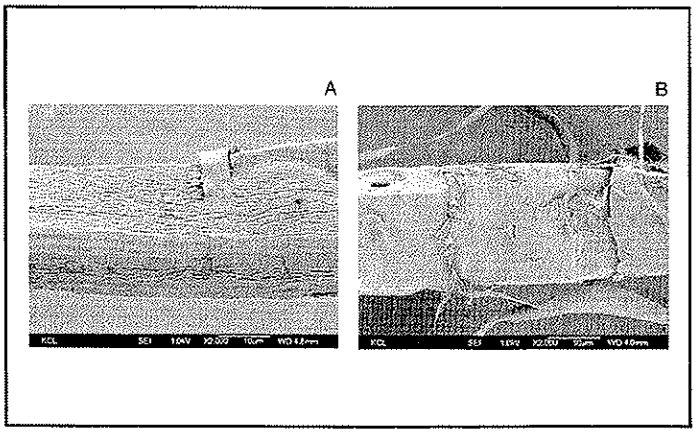

Fig. 3. FE–SEM images of TMP fibres (+14) after the first refining stage (A1).

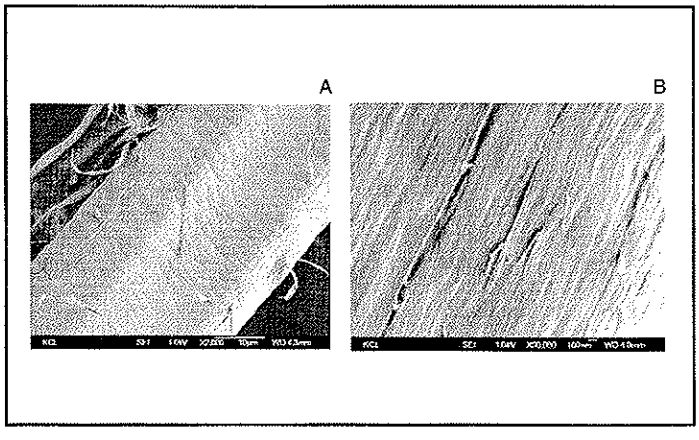

Fig. 4. FE–SEM images of TMP fibres after the first reject refining stage (B1).

Surface Structure of Fibres by FE–SEM

Images of the fibre surface after the first mainline refining stage (A1) are shown in Fig. 3. In Fig. 3A, a very wrinkled fibre surface caused by shrinkage can be seen. However, the fibril angle of this layer was perpendicular to the wrinkles and to the fibre axis. Thus it was deduced that this surface layer was an outer wall layer, consisting of P and S_1. The fibre corner in Fig. 3A looks very smooth, indicating the presence of a thick layer of middle lamella. Figure 3B shows the mechanism by which outer wall layers were peeled off the fibre surface. Because of the high fibril angle, it is seen often that outer wall layers come off in strips; the remaining outer wall layers were seen as bands surrounding the inner wall layers. This same mechanism is shown in images published previously [38].

Some images were also obtained at high magnification (X10 000–30 000) to examine the surface microstructure of the various fibre wall layers. Such images show the fibril angle more clearly, and therefore it should be possible to deduce the fibre wall layer in question (P, S_1, S_2 or S_3). Images of the fibre surface taken after the first reject refining stage (B1) are seen in Fig. 4, Fig. 4B being a high magnification of the surface in Fig. 4A. The fibre wall layer in the images is S_2, since the fibril angle is small. The fibrils have a tight structure, but some cracks have appeared between the fibril lamellae that may eventually lead to fibrillation.

Figure 5 shows images of the fibre surface after the second reject refining stage (B3). Figure 5A shows part of a fibre whose surface still retains some of the outer wall layers. However, it can be seen that the outer wall layer no longer is bonded tightly to the inner wall layer and that the fibre wall has started to delaminate. Also, it can be seen how fibrillar lamellae are formed at the boundary between the two layers. Such lamellae may contribute to the amount of flake-like fines in the pulp. The fibre in Fig. 5B has been split longitudinally. The fibre wall surface of S_3 towards the lumen had a clear fibrillar structure with fairly loose fibrils compared to the other fibre wall layers.

Manual FE–SEM measurement was used to determine how well the outer fibre wall layers (P+S1 including middle lamellae) had been removed during refining. The results (Fig. 6) show that, after the first mainline refining stage (A1), ~60% of the fibre length was already free from the outer fibre wall layers. During the second stage of refining (A2), a further 25% of the S_2 layer was revealed. This large increase in S_2 revealed in the second stage relates directly to the increased effect of energy on the fibre surface. After reject refining (B3), the fibres were fairly free of the outer fibre wall layers. A similar analysis was performed by Johnsen et al. [3]. Based on SEM images applying the backscatter imaging technique, they estimated that the area covered by middle lamellae was 24% of the total fibre surface area on TMP fibres after the first refining stage (pulp freeness 296 mL) and 15% on the final, screened pulp fibres (freeness 26 mL). They also concluded that S_2 covers most of the fibre surface area already after the first refining stage, which supports the results obtained in our work.

Surface Chemical Properties of Fibres and Fines by ESCA

ESCA was used to determine the coverage of lignin, extractives and polysaccharides on fibre surfaces (DDJ +200 fraction) (Fig. 7). The largest difference between the fibres from mainline and reject line refining was in the coverage of extractives on their surfaces, indicating that the extractives content decreased during screening. This was verified by determining the amount of acetone-extractable material in pulps before and after screening, in which case the decrease was from 1 to 0.2%. Prior to screening, the pulp was diluted to 1% consistency with tap water (pH 7.5–8) and hot disintegrated

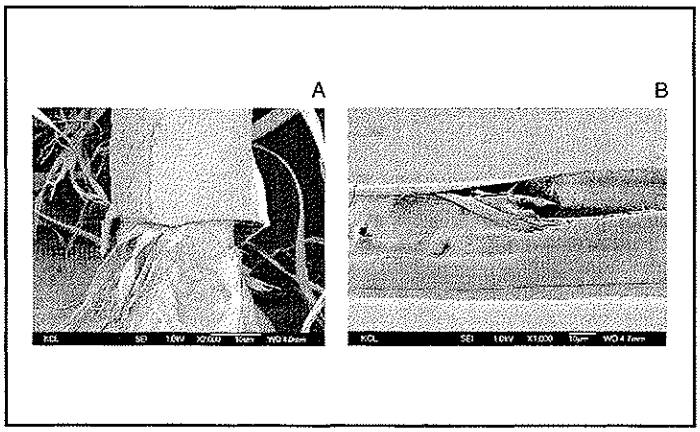

Fig. 5. FE–SEM images of TMP fibres after the second reject refining stage (B3).

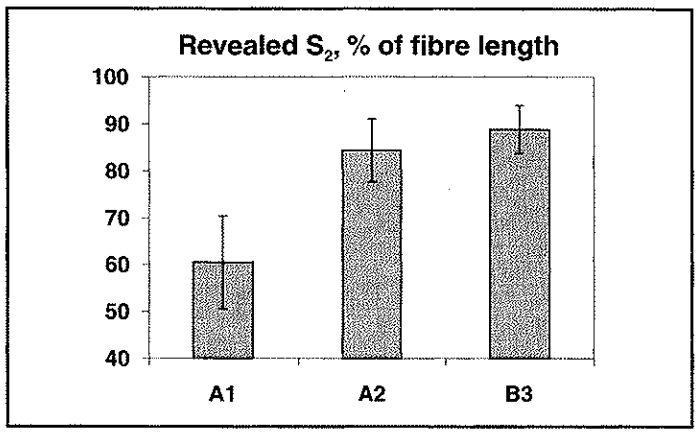

Fig. 6. Exposure of S_2 wall layer during the TMP process. A1 = after the first mainline refining stage (SEC 1.55 MWh/t), A2 = after the second mainline TMP refining stage (SEC 2.44 MWh/t), B3 = after the two-stage reject refining (SEC 4.65 MWh/t).

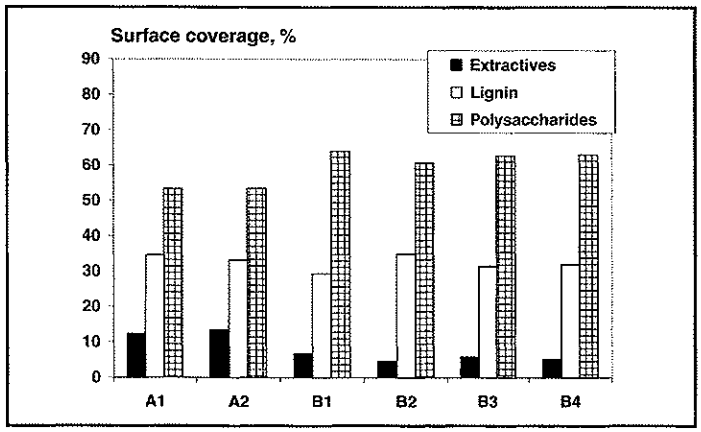

Fig. 7. The surface coverage of lignin, extractives and polysaccharides on fibres.

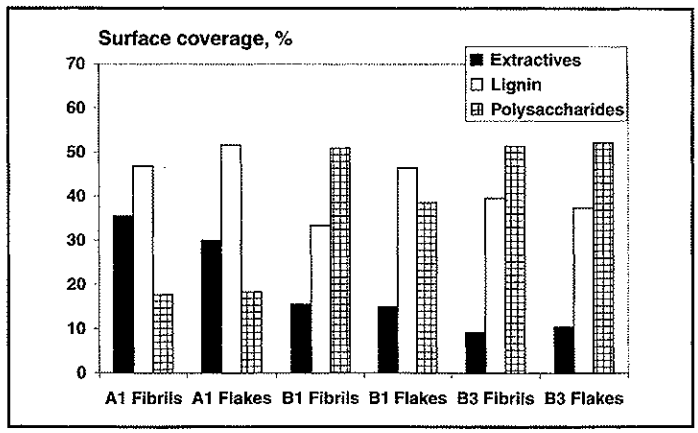

Fig. 8. The surface coverage of lignin, extractives and polysaccharides on fibrils and flakes.

at high temperature. The increase in temperature, pH and amount of water probably made the wood resin more soluble or dispersible and resulted in the washing of the extractives from the fibre surfaces. The screening also had an effect on the composition of the fibre fraction (DDJ +200), since part of the short fibres and material belonging to the middle fraction were removed with the accepts. This change in the composition of the fraction may have induced the change in the content of surface extractives, since most of the extractives may have been removed with the material in the accepts.

The surface coverage of lignin was slightly higher on fibres from mainline pulps than on those from reject line pulps, indicating that most of the lignin-rich middle lamella and outer fibre wall layers ($P+S_1$) had been removed by the end of the first reject refining stage. The decrease in the content of extractives and lignin on the fibre surfaces resulted in a corresponding increase in the surface coverage of polysaccharides, indicating that most of the cellulose-rich inner fibre wall layers had been exposed in fibres from the reject line, as was also observed by FE–SEM.

The surface chemical composition of fibrils and flakes also was analyzed with ESCA (Fig. 8). Similar changes were seen in the surfaces of both fines types as a function of refining energy. After the first mainline refining stage (A1), the fines were mostly covered with lignin and extractives. After the first (B1) and second (B3) reject refining stages, the extractives and lignin coverage had decreased and that of polysaccharides increased. The surface chemistry of fibrils and flakes was fairly similar after the second reject refining stage (B3).

The results show that both fibrils and flakes were formed throughout the refining process and that their surface chemical composition depended on their origin in the fibre wall. Fines rich in lignin were formed during the early stages of refining and those with more polysaccharide on their surfaces during reject refining. Fibrillar fines were probably first formed from the lignin-rich primary wall (P) and outer secondary wall (S_1) and, towards the end of refining, the content of secondary wall (S_1+S_2) fibrils increased. Flake-like fines formed during mainline refining probably consisted mainly of material from the middle lamella and primary wall. During reject refining, flakes from the outer wall layers, i.e. from $P+S_1$, were also released.

Surface Chemical Composition of Fibres by ToF–SIMS

ToF–SIMS can be operated in both negative and positive ion modes. Our previous results show that acidic extractives, i.e. fatty and resin acids, can be analyzed successfully in negative ion mode, whereas positive ion mode is preferred for neutral extractives such as triglycerides and sterols [20,39,40].

Part of the negative ToF–SIMS spectrum of TMP fibres (sample A1) is shown in Fig. 9. Based on an earlier model compound analysis [35], it is possible to identify peaks originating from the most commonly found extractives in Norway spruce from this spectrum. The peaks in the negative spectrum correspond to the molecular ion of the compound, which has lost a proton and acquired a negative charge ($[M-H]^-$ ion). The most abundant peaks at 279, 281 and 277 m/z originate from unsaturated fatty acids, namely linoleic, oleic and pinolenic acids, respectively. Smaller peaks at 255, 269, 283, 311 and 339 m/z can be assigned to the saturated fatty acids palmitic, anteisoheptadecanoic, stearic, arachidic and behenic acids, respectively. The resin acids dehydroabietic acid and abietic acid, along with its several isomers, can be seen at 299 and 301 m/z, respectively.

Part of the positive ToF–SIMS spectrum of TMP fibres (sample A1) is shown in Fig. 10. The peak with the highest intensity at 397 m/z originates from the molecular ion of sitosterol that has lost one hydroxyl group ($[M-OH]^+$ ion). Another intense peak at 383 m/z can be

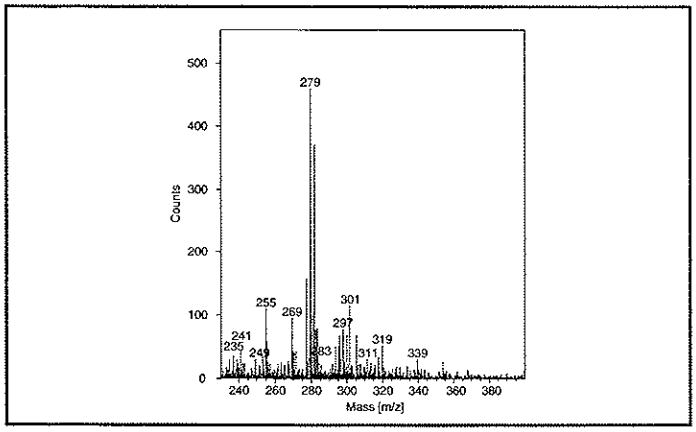

Fig. 9. Part of the negative ToF–SIMS spectrum of TMP fibres (sample A1).

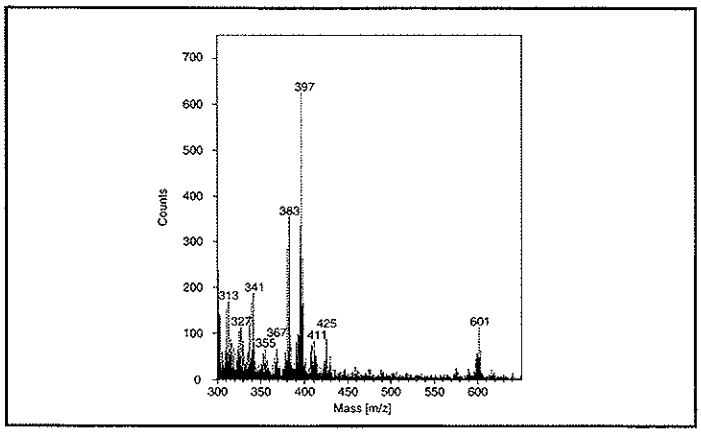

Fig. 10. Part of the positive ToF–SIMS spectrum of TMP fibres (sample A1).

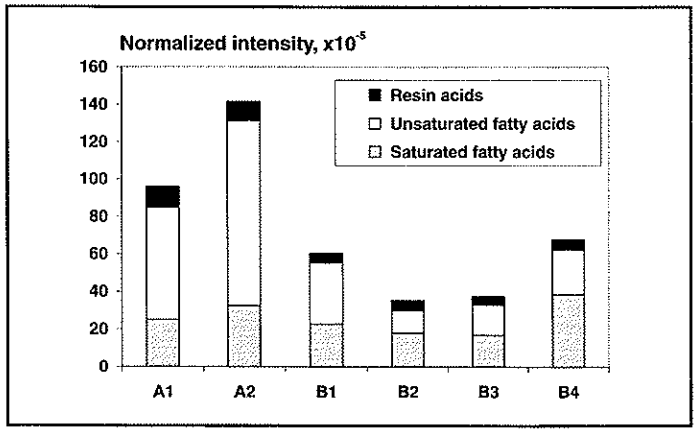

Fig. 11. Normalized intensities of acidic extractives on fibre surfaces. The values have been calculated from negative ToF–SIMS spectra.

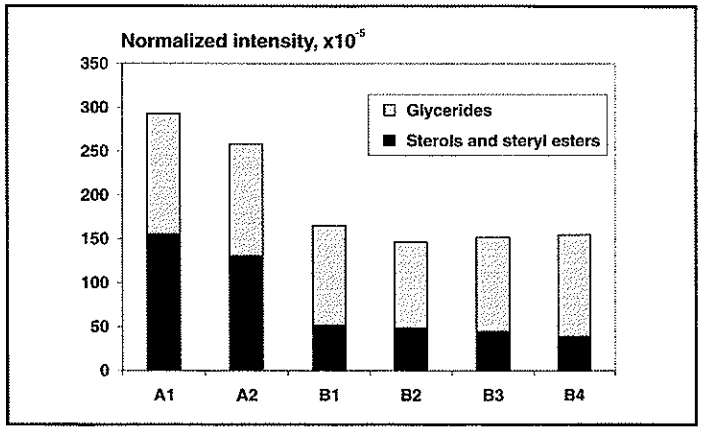

Fig. 12. Normalized intensities of neutral extractives on fibre surfaces. The values have been calculated from positive ToF–SIMS spectra.

assigned to campesterol. Peaks at 411 and 425 m/z originate from sterols and steryl esters. Triglycerides are very common wood resin components in Norway spruce [41]. No molecular ion peaks were seen for triglycerides at ~800 m/z, indicating that they have largely fragmented to smaller molecules during the ToF–SIMS analysis. The fragmentation pattern of triglycerides has been confirmed by model compound analysis [35,42]. The presence of triglycerides can be verified by looking at the peaks at ~340 m/z and at 600 m/z, the former representing monoglycerides and the latter diglycerides. When fragmented, fatty acid chains in triglycerides also give peaks corresponding to the molecular peaks of the free fatty acids, and so far it has been impossible to distinguish between esterified fatty acids and free fatty acids in ToF–SIMS spectra. This can be a serious difficulty when attempting to quantify using the ToF–SIMS method.

The amounts of various extractives on the surfaces of fibres were estimated by integrating the characteristic peak of each extractive in the ToF–SIMS spectra and by normalizing the peak intensity to the total intensity of the spectrum. The peaks were assigned to one of the following groups: unsaturated fatty acids; saturated fatty acids; resin acids; sterols and steryl esters; and glycerides and their values were added together. The method gives a semiquantitative indication of the relative amounts of various extractives and enables samples to be compared.

The normalized intensities of acidic extractives on fibre surfaces are shown in Fig. 11 and those of neutral extractives in Fig. 12. The contents of both these extractives were lower on the surfaces of fibres from the reject line than from the mainline. The reason was the dissolution or dispersion of extractives from the fibre surfaces during screening or their removal with the accepts, as explained above. According to the results, the relative amount of unsaturated fatty acids decreased more than that of other acidic extractives, indicating that they were more dispersible in water. Among the neutral extractives, the relative amount of sterols and steryl esters on fibre surfaces decreased more than that of glycerides. Käyhkö [43] found that acidic wood extractives, i.e. free fatty acids and resin acids, were transferred to the water phase to a lesser extent than neutral extractives, i.e. triglycerides and steryl esters, in the pulper after refining. Thus, our results suggest that the large decrease in the surface content of unsaturated fatty acids during the screening of pulp was due to a high content of unsaturated fatty acid chains in the released steryl esters.

Comparing the contents of surface extractives given by ESCA (Fig. 7) and ToF–SIMS (Figs. 11,12) shows that the results correlate well with each other in classifying the samples in the same order.

Gross Chemical Composition of Fibres, Fibrils and Flakes

The gross chemical composition was analyzed from the fractions of three pulp samples, namely from the pulp obtained after the first mainline refining stage (A1), after the first reject refining stage (B1) and after the second reject refining stage (B3).

The gross chemical compositions of TMP fibres, fibrillar fines and flake-like fines are shown in Fig. 13. The contents of hemicelluloses, i.e. mannan and xylan, and of pectins (i.e. galacturonans, arabinans and galactans), were obtained from the monosaccharide units given by acid methanolysis (Table III). The cellulose content was obtained from the glucose units given by acid hydrolysis (Table III). Many analyses are required to obtain all the chemical information shown in Fig. 13 and there are some losses that reduce the accuracy of the analysis. For this reason, the total amount shown for each fraction is often less than 100%. The monosaccharide composition of fibres and fines correlated well with results published previously [40,44].

The fibres contained mostly lignin, cellulose and glucomannan, the most common hemicellulose in spruce wood, but also some pectins, indicating that not all middle lamella or primary wall material was removed from their surfaces during the refining process. This agrees with the result obtained by FE–SEM (Fig. 6). The chemical composition of fibres changed only slightly during refining. Fibres from the mainline pulps contained more pectins and xylans than the reject line fibres, indicating that more middle lamella and outer fibre wall material was present on mainline fibres, since secondary wall contains no pectin [45,46]. The contents of cellulose and lignin stayed relatively constant in fibres during refining. The content of mannan was slightly lower in reject line fibres.

Flake-like fines were the most lignin-rich fraction. They also contained the lowest amount of glucomannan and cellulose. The pectin (rhamnogalacturonan, arabinan and arabinogalactan) and xylan contents of flakes were higher than those of the other fractions. Higher contents of galactan and arabinan have been found from middle lamella (ML) and primary wall (P) than from the secondary wall [45]. The compound middle lamella (ML+P) also has a lower content of cellulose and mannans than the secondary wall [45]. Ray cells are very rich in xylan and lignin [47].

The gross chemical composition of flake-like fines changed very little as refining progressed, indicating that they consisted mainly of ray cells and material originating from the compound middle lamella (ML+P). However, the changes observed in the surface

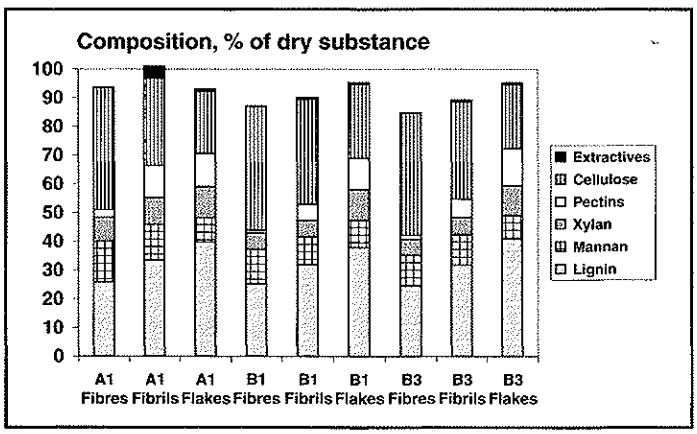

Fig. 13. Gross chemical compositions of TMP fibres, fibrils and flakes.

TABLE III
MONOSACCHARIDE COMPOSITION (mg/g) OF TMP FIBRES, FIBRILS AND FLAKES ANALYZED BY ACID METHANOLYSIS OR ACID HYDROLYSIS (GLUCOSE)

	Ara	Rha	Xyl	4-O-MeGlcA	Man	Gal	GalA	GlcA	Glc
A1									
Fibres	16	1.7	71	11	110	23	9.7	<1	500
Fibrils	33	6.3	79	11	96	52	46	1.3	361
Flakes	35	6.6	92	14	66	46	54	1.3	257
B1									
Fibres	9.6	1.0	50	8.0	93	14	2.8	<1	502
Fibrils	15	3.0	49	8.2	74	35	20	<1	424
Flakes	33	6.6	91	14	74	48	47	1.1	304
B3									
Fibres	9.9	1.1	48	9.4	83	17	3.7	<1	493
Fibrils	15	3.1	51	8.9	82	38	26	<1	395
Flakes	35	7.3	89	15	64	53	58	1.4	263

chemical composition of flakes (Fig. 8) indicate that the origin of the flake-like fines changed as refining proceeded. Initially, flakes originated probably from the middle lamella and primary wall while, later in the process, material from the outer secondary wall (S_1) was also included. The primary wall and the outer part of S_1 are known to be chemically similar, while the inner part of S_1 is similar in chemistry to S_2 [48]. Flakes from the inner S_1 may contain some lamellar structures originating from S_2, but microscopic studies have shown that flakes do not originate from S_2 itself. It could be that material from ML+P dominated in amount throughout the refining process and thus no differences were seen in the overall chemistry.

Fibrillar fines contained less lignin than flakes, but the content was still higher than in fibres. The cellulose, mannan and xylan contents of fibrils were also between those of fibres and flakes. The chemical composition of fibrils from mainline pulps differed from that of fibrils from the reject line. Fibrils after the first mainline refining stage (A1) had quite a high content of pectins (~10%), indicating that they originated at least partly from the primary wall. This is in agreement with earlier results on second stage TMP [40,47]. After the first reject refining stage (B1), the pectin content of fibrils had decreased by 50%, suggesting that the content of material originating from secondary wall in fibrils had increased.

The xylan content of fibrils behaved in a similar fashion to the pectin content, decreasing by almost 50% by the end of the first reject refining stage (B1). According to Meier [45], there is more xylan in the S_1 layer and inner secondary wall (part of S_2 and S_3) than in the compound middle lamella (ML+P) or the outer part of S_2. This supports further the conclusion that fibrils in the reject line pulps were released more from the outer part of S_2. The cellulose content of fibrils was slightly higher and the mannan content lower in the reject line pulps than in the mainline pulps.

The extractives content of fibrils after the first mainline refining stage was quite high. Wood resin dispersed or dissolved during pulping and subsequent process stages has probably re-adsorbed or deposited onto the fibril surface either during the pulping process or during fractionation [49]. Fibrillar fines have a high specific surface area [50] and can easily adsorb colloidal material. Mosbye et al. [19,51] agree that fines have a greater specific surface area than fibres and thus can adsorb more colloidal material. However, they claim that the adsorption of colloidal extractives onto fines depends on the chemical composition of the fines, and that the sterically stabilized colloidal extractives are more easily adsorbed onto lignin-rich flake-like fines than onto carbohydrate-rich fibrils. In our case, the fibrils obtained from mainline refining were similar in chemistry to flakes in that they had a high surface content of lignin. If chemistry is the dominant factor in adsorption behaviour, this might explain why fibrils from mainline refining had a high extractives content. However, the specific surface area of fines may affect the adsorption behaviour of colloidal pitch and not just their chemistry.

It was previously thought that fines originating from the middle lamella and primary wall of the fibre are flake-like particles and that fibrils originate from the secondary wall (S_1 + S_2) [52]. However, the results of the chemical analysis obtained in our work indicate that material classified as fibrillar according to the image analyzer originates from the primary wall as well. In addition, the changes occurring in the surface chemical properties of flake-like fines show that fines of this type can originate from the carbohydrate-rich secondary wall also.

CONCLUSIONS

The reduction in coarseness and fibre wall thickness indicated that material was peeled off the fibre surface during both mainline and reject refining. The increase in the content of fibrillar fines as well as in specific filtration resistance, indicated that a lot of well-bonding, i.e. fibrillar material, was generated during reject refining.

The surface morphology of fibres changed as refining proceeded. From ~60% of the secondary wall revealed in the first mainline refining stage, the percentage of visible S_2 layer covering the surface increased to over 80% in the second mainline refining stage. After the two-stage reject refining, 90% of the S_2 layer was revealed.

The largest difference between the mainline and reject line fibres was in the surface coverage of extractives. Extractives were mostly removed from fibres during screening. Among the acidic extractives on the fibre surface, the content of unsaturated fatty acids decreased the most, while sterols and steryl esters were found to be removed more than glycerides.

The surface coverage of lignin was lower on reject line fibres than on mainline fibres. Fibres from the reject line also had a higher polysaccharide content on their surface. Thus, the chemical results support the microscope results in suggesting that, in the reject line pulps, most of the lignin-rich outer fibre wall layers had been removed and more secondary wall had been exposed compared to the mainline fibres.

Both gross chemical and surface chemical analyses of fibrils indicated that the fibrils initially released originated from outer fibre wall layers, mainly P and S_1 but, at later stages, they were peeled off from the inner fibre wall layers (S_2) as well. The content of extractives was greatest in fibrils, indicating the adsorption or deposition of dissolved and colloidal pitch particles onto fibrillar surfaces.

During the early stages of refining, flake-like fines were formed from compound middle lamella (ML+P). As refining progressed, the surface chemical composition of flake-like fines changed, indicating a difference in their origin. More flakes were probably formed from the outer secondary wall (S_1) towards the end of refining.

In summary, high refining energies can be used to remove most of the lignin-rich outer fibre wall layers and to create fines with polysaccharide-rich surfaces. Screening aids in removing harmful pitch from the fibre surfaces.

ACKNOWLEDGEMENTS

We wish to thank Professor (Emeritus) Per Stenius for his valuable comments on this article. The authors would also like to thank Drs. Leena-Sisko Johansson and Joseph Campbell, Center for Chemical Analysis, Helsinki University of Technology, Espoo, Finland, for performing the ESCA analyses. Financial support from The Finnish Cultural Foundation is gratefully acknowledged.

REFERENCES

1. LIDBRANDT, O. and MOHLIN, U.-B., "Changes in Fibre Structure due to Refining as Revealed by SEM", Proc. Institute of Paper Chemistry Intl. Symp. Fund. Concepts of Refining, Appleton, WI, USA, 61–74 (1980).
2. CISNEROS, H.A., WILLIAMS, G.J. and HATTON, J.V., "Fibre Surface Characteristics of Hardwood Refiner Pulps", *J. Pulp Paper Sci.* 21(5):J178–J184 (1995).
3. JOHNSEN, P. O., SKINNARLAND, I., HELLE, T. and HOUEN, P. J., "Distribution of Lignin and Other Materials on Particle Surfaces in Mechanical Pulps", Preprints 1995 Intl. Mech. Pulping Conf., Tech. Sect., CPPA, 93–107.
4. GUSTAFSSON, J., CIOVICA, L., LEHTO, J.H., TIENVIERI, T. and PELTONEN, J., "The Influence of Defibration Temperature and Refining on the Surface Characteristics of Mechanical Pulps" in Research Techniques for Tomorrow's Papermaking. COST E11, Characterization Methods for Fibres and Paper, Final Workshop, Espoo, Finland, 67–70 (2001).
5. SNELL, R., GROOM, L.H. and RIALS, T.G., "Characterizing the Surface Roughness of Thermomechanical Pulp Fibres with Atomic Force Microscopy", *Holzforschung* 55(5): 511–520 (2001).
6. PENG, F. and JOHANSSON, L. "Characterization of Mechanical Pulp Fibres", *J. Pulp Paper Sci.* 22(7):J252–J257 (1996).
7. KARNIS, A., "The Mechanism of Fibre Development in Mechanical Pulping", *J. Pulp Paper Sci.* 20(10):J280–J288 (1994).
8. HEIKKURINEN, A. and HATTULA, T., "Mechanical Pulp Fines – Characterization and Implications for Defibration Mechanisms", Proc. 1993 Intl. Mech. Pulping Conf., PTF, 294–308.
9. LUUKKO, K., KAJOLA-KEMPPAINEN, P. and PAULAPURO, H., "Characterization of Mechanical Pulp Fines by Image Analysis", *Appita J.* 50(5):387–392 (1997).
10. BRAATEN, K.R., "The Impact of Fibre Geometry, Fibre Splitting and Fibrillation on Light Scattering", Proc. 1997 Intl. Mech. Pulping Conf., SPCI, 349–353.
11. REME, P.A., HELLE, T. and JOHNSEN, P. O., "Fibre Characteristics of Some Mechanical Pulp Grades", *Nordic Pulp Paper Res. J.* 13(4): 263–268 (1998).
12. DORRIS, G.M. and GRAY, D.G., "The Surface Analysis of Paper and Wood Fibres by ESCA. II. Surface Composition of Mechanical Pulps", *Cellul. Chem. Technol.* 12(6):721–734 (1978).
13. KOLJONEN, K., STENIUS, P. and BUCHERT, J., "The Surface Chemistry of PGW Pulp Fibre Fractions", Proc. 1997 Intl. Mech. Pulping Conf., SPCI, 407–411.
14. BÖRÅS, L. and GATENHOLM, P., "Surface Properties of Mechanical Pulps Prepared under Various Sulfonation Conditions and Preheating Time", *Holzforschung* 53(4):429–434 (1999).

15. PERE, J., LAPPALAINEN, A., KOLJONEN, K., TENKANEN, M. and MUSTRANTA, A., "Combination of Chemical and Immunomicroscopical Methods for Surface Characterization of Mechanical Pulp Fibres", Proc. 11th Intl.Symp. Wood Pulping Chem., ATIP, 1:259–262 (2001).
16. WESTERMARK, U., "The Content of Lignin on Pulp Fibre Surfaces", Proc. 10th Intl. Symp. Wood Pulping Chem., Japan TAPPI, 1:40–42 (1999).
17. MUSTRANTA, A., KOLJONEN, K., PERE, J., TENKANEN, M., STENIUS, P. and BUCHERT, J., "Characterization of Mechanical Pulp Fibres with Enzymatic, Chemical and Immunochemical Methods", Proc. 6th Euro. Workshop Lignocellulosics Pulp, ATIP, 15–18 (2000).
18. LUUKKO, K., LAINE, J. and PERE, J., "Chemical Characterization of Different Mechanical Pulp Fines", *Appita J.* 52(2):126–131 (1999).
19. MOSBYE, J., LAINE, J. and MOE, S., "The Effect of Dissolved Substances on the Adsorption of Colloidal Extractives to Fines in Mechanical Pulp", *Nordic Pulp Paper Res. J.* 18(1):63–68 (2003).
20. KLEEN, M., RÄSÄNEN, H., OHRA-AHO, T. and LAINE, C., "Surface Chemistry of TMP Fibres and Fines", Proc. 11th Intl. Symp. Wood Pulping Chem., ATIP, 255–258 (2001).
21. KANGAS, H., SALMI, J. and KLEEN, M., "Surface Chemistry and Morphology of Thermomechanical Pulp Fibres and Fines", Proc. 7th Euro. Workshop Lignocellulosics Pulp, PI, 115–118 (2002).
22. VANDER WIELEN, L.C. and RAGAUSKAS, A.J., "Dielectric Discharge: A Concatenated Approach to Fibre Modification", Proc. 12th Intl. Symp. Wood Pulping Chem., TAPPI PRESS, 1:373–376 (2003).
23. "Pulps. Laboratory Wet Disintegration", EN ISO 5263, Intl. Org. Standardiz., Geneva, Switzerland (1997).
24. "Pulps – Determination of Dry Matter Content", EN ISO 20638, Intl. Org. Standardiz., Geneva, Switzerland (1993).
25. "Pulps – Determination of Drainability – Part 2. Canadian Standard Freeness Method", ISO 5267-2, Intl. Org. Standardiz., Geneva, Switzerland (2001).
26. "Fibre Fractionation of Mechanical Pulp in the McNett Apparatus", Test Method SCAN-M 6:69, Scandinavian Pulp, Paper and Board Testing Comm., Stockholm, Sweden (1969).
27. "Determination of Acetone-Soluble Matter", Test Method SCAN-CM 49:93, Scandinavian Pulp, Paper and Board Testing Comm., Stockholm, Sweden (1993).
28. "Acid-Insoluble Lignin in Wood and Pulp", TAPPI Test Method T 222 (1998).
29. "Carbohydrate Composition of Extractive-Free Wood and Wood Pulp by Gas-Liquid Chromatography", TAPPI Test Method T 249 (2000).
30. SUNDBERG, A., SUNDBERG, K., LILLANDT, C. and HOLMBOM, B., "Determination of Hemicelluloses and Pectins in Wood and Pulp Fibres by Acid Methanolysis and Gas Chromatography", *Nordic Pulp Paper Res. J.* 11(4):216–219, 226 (1996).
31. LAINE, C., TAMMINEN, T., VIKKULA, A. and VUORINEN, T., "Methylation Analysis as a Tool for Structural Analysis of Wood Polysaccharides", *Holzforschung* 56(6):607–614 (2002).
32. SJÖSTRÖM, E., Wood Chemistry – Fundamentals and Applications, 2nd ed., Academic Press, San Diego, CA, USA (1993).
33. WILLFÖR, S., SJÖHOLM, R., LAINE, C. and HOLMBOM, B., "Structural Features of Water Soluble Arabinogalactans from Norway Spruce and Scots Pine Heartwood", *Wood Sci. Technol.* 36(2):101–110 (2002).
34. KLEEN, M., SJÖBERG, J., DAHLMAN, O., JOHANSSON, L.-S., KOLJONEN, K. and STENIUS, P., "The Effect of ECF and TCF Bleaching on the Chemical Composition of Soda-Anthraquinone and Kraft Pulp Surfaces", *Nordic Pulp Paper Res. J.* 17(3):357–363 (2002).
35. KANGAS, H. and KLEEN, M., "The Effect of Peroxide Bleaching on the Surface Chemical Composition of Mechanical Pulps", Proc. 12th Intl. Symp. Wood Pulping Chem., TAPPI PRESS, 1:381–384 (2003).
36. MANNSTRÖM, B., "On the Characterization of Mechanical Pulps", Proc. 1968 Mech. Pulping Conf., TAPPI PRESS, 35.
37. LUUKKO, K. and PAULAPURO, H., "Mechanical Pulp Fines: Effect of Particle Size and Shape", *Tappi J.* 82(2):95–101 (1999).
38. MOSS, P. and HEIKKURINEN, A., "Swelling of Mechanical Pulp Fibre Walls Studied by CLSM", Preprints 2003 Intl. Mech. Pulping Conf., PAPTAC, 293–297.
39. KLEEN, M., KANGAS, H. and KRISTOLA, J., "Surface and Bulk Chemical Properties of Groundwood Pulp Fibres and Fines", Proc. 7th Euro. Workshop Lignocellulosics Pulp, PI, 447–450 (2002).
40. KLEEN, M., KANGAS, H. and LAINE, C., "Chemical Characterization of Mechanical Pulp Fines and Fibre Surface Layers", *Nordic Pulp Paper Res. J.* 18(4):361–368 (2003).
41. EKMAN, R., "Analysis of the Nonvolatile Extractives in Norway Spruce Sapwood and Heartwood", *Acta Acad. Aboensis, Ser. B* 39(4):1–15 (1979).
42. KLEEN, M. and NILVEBRANDT, N.-O., "Simultaneous Characterization of Free and Esterified Fatty Acid Salts Using Time-of-Flight Secondary Ion Mass Spectrometry", Post-Symp. Workshop 11th Intl. Symp. Wood Pulping Chem., ATIP, 51–54 (2001).
43. KÄYHKÖ, J., "The Influence of Process Conditions on the Deresination Efficiency in Mechanical Pulp Washing", PhD Thesis, Lappeenranta Univ. Technol., Dept. Chem. Technol., Lappeenranta, Finland (2002).
44. SUNDBERG, A., PRANOVICH, A.V. and HOLMBOM, B., "Chemical Characterization of Various Types of Mechanical Pulp Fines", *J. Pulp Paper Sci.* 29(5):173–178 (2003).
45. MEIER, H., "General Chemistry of Cell Walls and Distribution of the Chemical Constituents Across the Walls" in The Formation of Wood in Forest Trees, M.H. Zimmerman, Ed., Academic Press, New York, NY, USA, 137–151 (1964).
46. HAFREN, J., "Ultrastructure of Wood Cell Wall", PhD Thesis, Royal Inst. Technol., Dept. Biotechnol., Stockholm, Sweden (1999).
47. WESTERMARK, U., HARDELL, H.-L. and IVERSEN, T., "The Content of Protein and Pectin in the Lignified Middle Lamella/Primary Wall from Spruce Fibres", *Holzforschung* 40(2):65–68 (1986).
48. PANSHIN, A.J. and DE ZEEUW, C., "The Woody Plant Cell" in Textbook of Wood Technology, 3rd ed., McGraw-Hill, New York, NY, USA, 67–109 (1970).
49. ALLEN, L.H., "Characterization of Colloidal Wood Resin in Newsprint Pulps", *Colloid Polym. Sci.* 257:533–538 (1979).
50. WOOD, J.R., GRONDIN, M. and KARNIS, A., "Characterization of Mechanical Pulp Fines with a Small Hydrocyclone. Part I: The Principle and Nature of the Separation", *J. Pulp Paper Sci.* 17(1):J1–J5 (1991).
51. MOSBYE, J., LAINE, J. and MOE, S.T., "Adsorption of Colloidal Extractives to Different Types of Fines", Proc. 12th Intl. Symp. Wood Pulping Chem., TAPPI PRESS, 1:93–96.
52. MOHLIN, U.-B., "Fibre Development during Mechanical Pulp Refining", *J. Pulp Paper Sci.* 23(1):J28–J33 (1997).

REFERENCE: KANGAS, H., PÖHLER, T., HEIKKURINEN, A. and KLEEN, M., Development of the Mechanical Pulp Fibre Surface as a Function of Refining Energy, Journal of Pulp and Paper Science, 30(11):298–306 November 2004. Paper offered as a contribution to the Journal of Pulp and Paper Science. Not to be reproduced without permission from the Pulp and Paper Technical Association of Canada. Manuscript received March 31, 2004; revised manuscript approved for publication by the Review Panel October 14, 2004.

KEYWORDS: THERMOMECHANICAL PULPS, PICEA ABIES, REFINING, ENERGY CONSUMPTION, FIBER STRUCTURE, SURFACE PROPERTIES, FINES, REJECTS, EXTRACTIVES.